Lithuanian Journal of Physics, Vol. **55**, No. 2, pp. 100–109 (2015)

NONLINEAR PROPERTIES OF SILVER NANOPARTICLES EXPLORED BY A FEMTOSECOND Z-SCAN TECHNIQUE

A. Alesenkov [a], J. Pilipavičius [b], A. Beganskienė [b], R. Sirutkaitis [c], and V. Sirutkaitis [a]

[a] *Laser Research Center, Vilnius University, Saulėtekio 10, LT-10223 Vilnius, Lithuania*

[b] *Department of Inorganic Chemistry, Vilnius University, Naugarduko 24, LT-03225 Vilnius, Lithuania*

[c] *Institute of Biochemistry, Vilnius University, Mokslininkų 12, LT-08662 Vilnius, Lithuania*

E-mail: aleksandr.alesenkov@ff.vu.lt

Received 10 February 2015; revised 22 April 2015; accepted 15 June 2015

In this report we present results of linear and nonlinear optical properties of colloidal material consisting of triangle silver nanoparticles in distilled water. The nonlinear optical properties of the material were investigated by a Z-scan technique using femtosecond laser pulses with tunable wavelength. Nanoparticle suspension showed distinct spectra with absorption lines, emerging due to the plasmonic properties of the silver nanoparticles. Surface plasmon resonance peak change over a wide range of wavelengths from 400 to almost 1100 nm was observed when the size of silver nanoparticles varied from 20 to 150 nm. In the samples different nonlinear effects such as saturable absorption, two photon absorption and self-focusing were observed when the femtosecond pulse intensity was changed from 1 up to 100 GW/cm^2.

Keywords: Z-scan, silver nanoprism, two-photon absorption

PACS: 42.65.Jx

1. Introduction

Nanoparticles exhibit many interesting linear and nonlinear properties, which are mainly related to the surface plasmons as the percentage of surface atoms in nanoparticles is huge compared to that in bulk materials. Therefore nanoparticles as a form of solid substance are the best catalysts [1], however, they also strongly influence optical parameters of composite materials. Resonance conditions for surface plasmons of metal nanoparticles can be easily tuned in a wide optical range by changing the nanoparticle size and morphology, material composition or even surrounding media [2, 3]. A great deal of recent scientific interest is concentrated in the field of laser–matter interaction [4] and the underlying physical phenomena, where optical fields tune the properties of the matter and the response becomes nonlinear. The natural interest in metal nanoparticales, nanoapertures in metal films, and metamaterials comes from the possibility of enhancing local electromagnetic fields which can enormously facilitate weak nonlinear light–matter interactions [6, 7]. In some predictions enhancement factors are 10^3–10^6 compared to the fundamental electric field at a flat metal surface. Due to these prominent features such as tuning of light–matter interaction strength in the case of nanoparticles made of highly conductive material, nanoparticles are not only widely studied [8–10] but also already applied in various fields such as nanobiosensors in disease treatment [11, 12], as absorptive, fluorescent or scattering optical sensors in biology [12, 13].

Recent technologies like photochemistry and wet chemistry have enabled fabrication of dozen various nanoparticles with different shapes and a controlled size. A wide variety of shapes have been realized for various compositions including Au (cubes and tetrapods [14], prisms [15], rods [16]), Pt (cubes, tetrahedral [17]) and Ag (wires [18], rods [13, 19], belts [20], plates [21]). Particularly successful is the production of nanospheres, nanorods and nanotriangles with a well-controllable edge length and tight size distribution maintenance [21–23]. There have been numerous reports on linear and nonlinear optical properties for various nanoparticles. However, the majority of those studies focus on the optical response of nanoparticles at the wavelength which corresponds to either in-plane dipole or in-plane quadrupole surface plasmon resonance (SPR) peak.

In this report we describe the production steps as well as linear and nonlinear optical characterization of nanocomposite silver colloids in the near infrared

spectral region. Silver nanoprisms were synthesized in an aqueous solution by a seed-mediated method [24]. Using this technique, we produced several nanocomposite materials, containing different size silver nanoparticles with a prismatic or truncated triangular shape. Note that anisotropic nanoparticles, particularly those with sharp points such as triangular nanoprisms, produce much stronger electric fields than simple structures such as nanospheres, therefore anisotropic nanoparticles are of particular interest for nonlinear optics. The outcome of the growth process was analyzed and characterized by means of conventional microscopy, dynamic light scattering (DSL), absorption spectroscopy (AS) and scanning electron microscopy (SEM). By means of degenerate femtosecond Z-scan nonlinear properties of the silver nanoprisms have been investigated in the near infrared (NIR) spectral region including the telecommunication wavelength at 1300 nm, paying particular attention to the third-order nonresonant electronic nonlinearities as they exhibit the fastest time response.

2. Experiment

2.1. Synthesis of silver nanoprisms

Different size (edge length) triangular silver nanoparticles were synthesized via the two-step seed-mediated growth procedure described below.

Seed production. A stock water solution of silver nanoparticles was produced by a reduction reaction of silver nitrate with sodium borohydride. A typical procedure based on a combination of aqueous trisodium citrate (trisodium 2-hydroxypropane-1,2,3-tricarboxylate 5 mL, 2.5 mM), aqueous sodium polystyrenesulphonate (PSSS; 0.25 mL, 500 mg/L; 1000 kDa), and aqueous sodium borohydride ($NaBH_4$ 0.3 mL, 10 mM, freshly prepared, added by drip) was performed. The procedure was followed by addition of aqueous silver nitrate ($AgNO_3$ 5 mL, 0.5 mM) at a rate of 2 mL/min, while cooling in an ice bath and under continuous magnetic stirring. A bright yellow solution was produced in the end and was stored in the dark. The colloid solution was stable for a few months.

Nanoprism growth. The nanoprisms were produced by combining 5 mL of distilled water (ultrapure deionized water with a resistivity of >18 MΩ cm), aqueous ascorbic acid ((5*R*)-[(1*S*)-1,2-dihydroxyethyl]-3,4-dihydroxyfuran-2(5*H*)-one 75 mL, 10 mM), and various quantities of the seed solution prepared earlier. This was followed by addition of aqueous silver nitrate (3 mL, 0.5 mM) dropwise at a rate of 1 mL/min. After the synthesis aqueous trisodium citrate (0.5 mL, 25 mM) was added to stabilize the particles. All chemicals were used without further purification as obtained from *Sigma-Aldrich* or *Merck*. All the glassware used were cleaned with a freshly prepared aqua regia solution (HCl/NO_3, 3:1) and then rinsed thoroughly with ultrapure water.

2.2. Characterization of the linear optical properties of nanomaterials and particle sizes

The detailed characterization of linear optical properties as well as the nanoparticle size characteristics were obtained by UV–VIS–NIR spectroscopy along with dynamic light scattering (DSL) and SEM. The linear absorption spectra were measured by a scanning spectrophotometer Shimadzu UV-3101 in the spectral range between 190 and 1400 nm. The average size as well as size dispersion and nanoprism shape were characterized by DSL (Zetasizer from *Malvern Instruments Ltd*) and SEM (scanning electron microscope). Micrographs of the nanoparticles were obtained with a Hitachi TM-1000 (Tokyo, Japan) microscope without using any conductive overlayer. Nanoparticles were dried on a glass substrate. DSL measurements were undertaken several times at the same conditions to confirm the chemical as well as aggregational stability of the colloids. The same instrument, the same ambient temperature (25 °C) and nanoparticle concentration were used in all experiments. The obtained translational diffusion coefficient did not vary for the same suspensions, which indicated that hydrodynamic radius of the nanoparticles does not change over time. The cause for that achievement is the proper selection of the capping agent (trisodium citrate) which prevents the agglomeration of the nanoparticles in the suspension by providing the negative charge to the nanoparticles due to the adsorbed citrate ions. A repulsive force works along the particles and prevents the agglomeration. However, after a few hours in the samples with the biggest nanoprisms they tend to precipitate and gather at the bottom. Therefore all the suspensions were thoroughly stirred before experiments and they were held in such conditions that the precipitation will not affect experiment results during the Z-scan measurements which for the fixed beam energy took only 5 minutes.

2.3. Characterization of the nonlinear optical properties

Nonlinear properties of silver nanoprisms were analyzed by means of the femtosecond degenerate Z-scan

technique [5, 25] taking into account many considerations proposed in [26]. Measurements were made at several wavelengths in the NIR spectral region. In this technique one measures the nonlinear phase front distortion induced in a sample by a focused beam passing through it. The phase front distortion is represented as optical transmittance variation through an aperture placed in the transmitted beam path which is a function of the sample distance from the beam waist. All measurements were performed using femtosecond pulses from an optical parametric generator/amplifier (OPG/OPA, *Light Conversion Ltd.*, model TOPAS), providing ~100 fs pulses tunable in the wavelength range from 300 to 2400 nm. A Ti:sapphire femtosecond laser (Vitara oscillator and Libra regenerative amplifier, *Coherent*) served as a pump source for the OPG/OPA. The pump pulse duration was 98 fs with a bandwidth of 16 nm centered at 798 nm. The repetition rate was set to 1 kHz, which excluded any thermal contribution to the measured nonlinear absorption/refraction signal. So any thermal lensing or other thermal effects were not expected in the sample. The signal pulse beam from OPG/OPA tunable in the spectral range 1100–1580 nm used for experiments after parametric conversion was spectrally cleaned from idler radiation (1600–2600 nm) by a pair of dichroic mirrors and spatially cleaned to follow a Gaussian distribution by focusing into a pinhole. The quality factor of the used femtosecond beam measured after parametric conversion, wavelength separation and spatial cleaning was quite low (M^2 = 1.25), which is sufficient to make an assumption that the beam is ideally Gaussian. Then the beam was recollimated and translated to the experimental area, where it was focused by a 300 mm focal length lens to produce the spot size of approximately w_0 = 40 μm at the focal plane. For the pulse energy of E = 1 μJ, this results in an on-axis light intensity of up to I_0 = 330 GW/cm^2. Liquid samples were contained in the quartz cuvette (SUPRASIL, UVFS from *Fisher Scientific*). During the measurements, the cuvette with the suspension inside was translated along the beam focal region and the whole or diaphragmed transmitted beam far-field intensity pattern was monitored by large area germanium photodetectors. The signal from the diaphragmed detector is related with nonlinear refraction, whereas the undiaphragmed signal is related with nonlinear absorption. Linear absorption spectra of each sample were routinely checked after the irradiation with high intensity (above 10 GW/cm^2) laser field and compared with the spectrum before laser irradiation. This was done to ensure nanoparticle integrity and suspension stability.

The SPR peak wavelength of the used nanoparticle suspensions is shorter compared to the excitation wavelength. After considerations of the absorption spectra and exciting photon energy the nonlinear response in the experiment was expected to be of the third order. Therefore we used a numerical Gaussian decomposition method [5, 25, 27–29] to extract the third-order nonlinear refraction coefficient (n_2). To model and fit experimental data of nonlinear absorption the model accounting for linear (in terms of effective sample length) as well as two-photon absorption was used. To verify the whole measurement procedure of our Z-scan setup nonlinear refraction of the fused silica plate (0.27 cm^2/PW at 1300 nm) and two-photon absorption of thin GaAs samples (16 cm/GW at 1300 nm) were used. The results were found to fit within 10% inaccuracy of the reported values of other groups. It should be mentioned that for measurement of such small nonlinear refraction much higher intensities (>500 GW/cm^2) of the beam were required, in comparison with the intensities used in the experiments with nanoparticle suspensions.

During the experiment, the silver nanoparticles were surrounded by water (n = 1.33, 1 mm thickness). Colloids were bounded by high quality fused silica cell borders (n = 1.46, border width 1 mm). These facts, which influence electromagnetic field intensity due to Fresnel reflections from media boundaries, were included in the theoretical model. However, we ignored nonlinear contribution from silica cells and water because the transmission variation signal from the pure water cell was under the noise threshold even at high excitation intensities (~50 GW/cm^2). Therefore, any nonlinear signal obtained from the experiment was attributed to the nonlinear response of silver nanoparticles.

Nonlinear absorption of each sample was measured by the open aperture Z-scan method. The normalized sample open aperture transmittance T_{OA} can be described by Eq. (1) [25]:

$$T_{OA}=\frac{1+(z/z_R)^2}{2\sqrt{\pi\Delta\Phi}}\int_{-\infty}^{\infty}\ln\left(1+\frac{2\Delta\Phi}{1+(z/z_R)^2}\cdot e^{-\tau^2}\right)d\tau, \quad (1)$$

where $\Delta\Phi = 2\cdot\beta/(I\cdot L_{eff})$ is the wave front distortion induced by nonlinear absorption, I is the on-axis peak irradiance at the focal plane, z_R is the Rayleigh length of Gaussian incident beam, $L_{eff} = [1 - \exp(-\alpha L)]/\alpha$ is the sample effective thickness and α is the linear absorption length.

Each sample nonlinear refraction was measured using the closed aperture Z-scan method. The normalized transmittance of the closed aperture Z-scan for a sample was fitted to the numerical model, which assumes that the distorted Gaussian beam passed

through nonlinear media can be presented as a sum of Gaussian beams with certain related parameters [5, 25, 27–29]. From the fit model the wave front phase distortion related to nonlinear refraction is derived, which is proportional to the nonlinear refraction index:

$$n_2 = \sqrt{2}\,\frac{\Delta\Psi}{l\cdot k\cdot L_{\text{eff}}}[\text{m}^2/\text{W}], \qquad (2)$$

where $\Delta\Psi$ is the maximal on-axis wave front phase distortion on the sample exit plane, I is the on-axis intensity of electromagnetic wave at the focal plane, k is the wave number and L_{eff} is the sample effective thickness.

3. Results and discussion

The main parameters of the used in the experiments seven colloidal materials consisting of triangle silver nanoparticles in distilled water are presented in Table 1: the average size, main plasmonic absorption band and size dispersion of Ag nanoparticles. As can be seen, the average size of the nanoparticles varied from 36 to 190 nm with the distribution size dispersion from 37 to 290 nm and it influenced the shift of the main absorption peak from 516 to 1040 nm. FWHM of the main absorption band also increased with the main peak shifting to longer wavelengths.

The explicit size distribution of silver nanoparticles measured by the DLS technique for samples S1, S4 and S7 are presented in Fig. 1. It also shows that dimensions of the grown nanoparticles are distributed in a wide range. For example, nanoparticles with the smallest average size equal to 36 nm

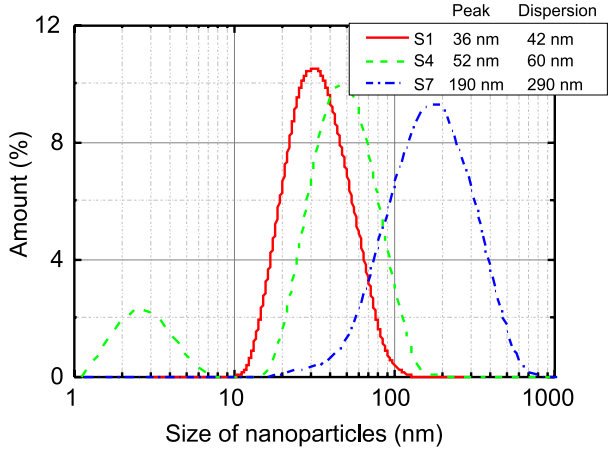

Fig. 1. Size distribution of the silver nanoparticles measured by the DLS technique for samples S1, S4 and S7. Distribution peak and size dispersion (denoted as Peak and Dispersion) analysis is also shown.

are distributed in the range from 11 to 110 nm. SEM micrographs of dried suspension on a glass substrate showed that nanoprisms tend to agglomerate and stack (face to face) over each other when drying. This was also the drawback to investigate the nanoparticles by electron transmission microscopy. However, agglomeration was utilized to estimate the particle thickness. Thus, the average silver nanoprism edge length varied from 36 to 190 nm in different samples. Specifically, the edge length distribution in our polydispersed samples spanned from 42 nm in sample S1 to 290 nm in sample S7. For experiments the usage of nanoprisms with an identic size is preferable, however, our synthesis scheme cannot yield particles with the size distribution to less than ±55%. The thickness of nanoprisms varied from 3 nm in S1 to 16 nm in S7, respectively. The absorption peak for different samples correlated with the nanoparticle size obtained from DLS measurements (Fig. 1 and Table 1).

Table 1. The average size, main plasmonic absorption band and size dispersion of the Ag nanoparticles used in experiments.

Sample	Main SPR absorption peak, nm	FWHM of the main absorption band, nm	Distribution size peak, nm	Distribution size dispersion, nm
S1	516	114	36	42
S2	570	135	39	37
S3	636	155	45	47
S4	717	195	52	60
S5	820	292	106	150
S6	1052	414	111	194
S7	1040	813	190	290

The main resonance in the absorption spectrum is found to be very intense and easily recognizable on the nearly flat transmission plateau of the deionized water up to the strong absorption peak at 1453 nm. Absorption spectra for all used examples in the UV–VIS–NIR spectral range are presented in Fig. 2. These intense peaks were at 516, 717 and 1040 nm for samples S1, S4 and S7, respectively. Spectrum profiles are broad and asymmetric with FWHM from 114 to 813 nm. For example, for sample S4 the resonance peak is spanning from 320 to 1100 nm. With the increasing of the nanoparticle growth time, broadening and shift of the main absorption peak to the red part of the spectrum was observed (see Table 1). These main peaks

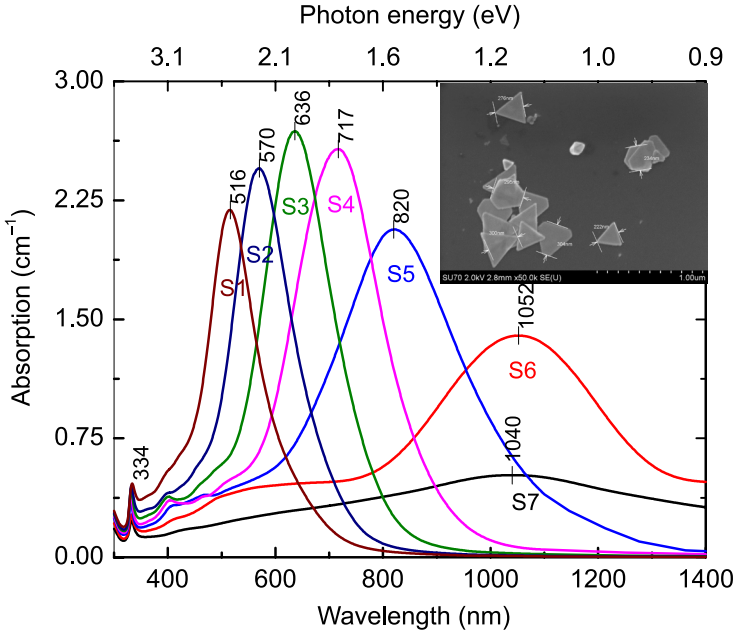

Fig. 2. UV–VIS–NIR absorption spectra of Ag nanoprisms of different size in water. Inset: SEM micrograph of the biggest silver nanoprisms dried on glass substrate.

correspond to in-plane dipole resonances [30]. They arise from the collective oscillation of the free electrons of the metal nanoparticles and are called surface plasmons or the Mie resonance in response to the electromagnetic field of characteristic frequency. The position of these peaks is sensitive to particle geometrical dimensions, such as the triangular nanoprism edge length and height, metal anisotropy and the dielectric constant of metal as well as surrounding media. However, it should be noted that the observed peaks are broadened. The absorption peak width is determined by dispersion of particle geometrical dimensions as well as by nanoparticle tip sharpness [31]. More detailed absorption spectra analysis also revealed the existence of much weaker in-plane quadrupole resonances hidden in the wings of the main resonance (peak wavelength of 423 and 395 nm for sample S1, 453 and 423 nm for sample S2, 489 and 458 nm for sample S3, 509 and 463 nm for sample S4). They arise due to phase retardation effects in the collective surface electron oscillations in light–matter interaction in response to the electrical field. This means that the diameter of the nanoparticles is big compared with the skin depth $(d = \lambda/4\pi\sqrt{\varepsilon})$, where ε is the dielectric constant of silver) and indeed the electrons oscillate not in unison across the particle. The shortest wavelength resonance at 334 nm is invariant for all samples. This indicates that it is the out-of-plane quadrupole resonance. The shoulder appearing below 320 nm indicates the onset of interband transition for silver crystal. The main absorption peaks of the spectra were not changing their spectral position over the time (several measurements during a week), which confirmed the stability of the suspensions.

The nonlinear transmission experiments showed that the silver nanoparticles with SPR peaks in the near infrared (samples S6 and S7) under 1200 nm excitation experienced the significant increase in optical transmission at high excitation intensity in contrast to low intensity excitation, when the optical transmission was lower (see Fig. 3). Here, the open circles denote experimental data and the solid line is a theoretical fit of the above mentioned model. The open aperture transmission shows a peak, symmetric around the beam focus position, where the laser pulse has the largest on-axis

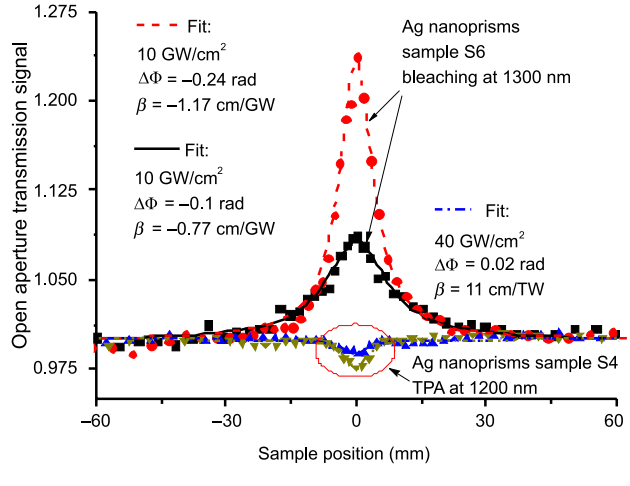

Fig. 3. Experimental normalized open aperture transmission data (dots) and theoretical fits (lines) of AgNP samples S4 and S6 at different beam intensities showing negative and positive nonlinear absorption, respectively. Beam characteristics: pulse duration 98 fs, wavelength 1200 and 1300 nm, beam width at focal plane 41 and 54 μm at 1/e^2.

fluence (on-axis peak fluence is denoted on the figures). The open aperture peak results in the negative nonlinear absorption coefficient β, known to be the saturated absorption (SA) signature. Such transmission behaviour is considered to be induced by ground-state-bleaching and interband transitions in silver nanoparticles. Similar OA transmission behaviour was already observed in the study of silver nanorods with picosecond laser radiation [32], silver nanospheres [33] and gold-silver nanoplanets [34] with femtosecond laser pulses. Although the theoretical model accounts for the linear absorption through the effective length of a sample, single-photon transitions at this excitation wavelength in samples S7 and S6 could have a significant influence on the absorption signal, as the sample linear transmission at this wavelength was quite low (only ~15%). It should be mentioned here that the size dispersion as well as the corresponding absorption line width for the samples with the biggest nanoparticles were broadest as was explored by the DSL measurements. Silver nanoparticles in sample S6 had the nonlinear absorption coefficient of –0.3 cm/GW at 1200 nm and this value decreased more than twice (–0.88 cm/GW) when the excitation wavelength was switched to the telecommunication wavelength of 1300 nm (Fig. 4(a)). The water absorption peak at 1450 nm did not allow to properly evaluate the nonlinear absorption of nanoprisms at longer wavelength (1400–1600 nm) as the weak beam depletion assumption was no longer valid at these experimental conditions. However, the order of measured nonlinearities is consistent with the results obtained by Wang et al. [35] (β from 0 to –3.2 cm/GW), although they used different wavelength (735 nm), pulse width (2.5 ps), repetition rate (76 MHz) and aimed to study the nonlinear optical response near the SPR peak of silver nanoplates.

Samples S3 and S4 showed different absorptive behaviour (Fig. 4(b)). Thus, the open aperture Z-scan traces for these samples showed a dip in an optical transmission curve at the beam focal plane, where the beam intensity is highest. The peak is symmetric and it indicates the increased absorption for the high beam intensities. The third-order absorption model accounting for two-photon absorption fits the curve almost perfectly and the absorption coefficient does not depend on the excitation field. This signifies that in these samples the TPA process is dominant. The degenerate nonlinear absorption coefficient is calculated to be 5 cm/TW for sample S3, whereas it was almost doubled (9.7 cm/TW) for sample S4 when the beam wavelength was 1200 nm. Similar (positive) nonlinear absorption was observed by antiresonant ring interferometric nonlinear spectroscopic techniques in silver colloids with spherical nanoparticles with the femtosecond laser excitation (100 fs, 730–800 nm) in the spectral range corresponding to the doubled wavelength of quadrupole plasmonic resonance [34]. In this study, nonlinear absorption was accounted for TPA by the quadrupole surface plasmon.

Nonlinear refraction reflects typical closed aperture transmission curves which are shown in Fig. 5. Dots denote experimental data and the solid line is a theoretical fit. In our experiment, the close aperture Z-scan transmission curve in samples S3–S5 shows a typical asymmetric "valley followed by the peak", known to be a signature of positive nonlinear

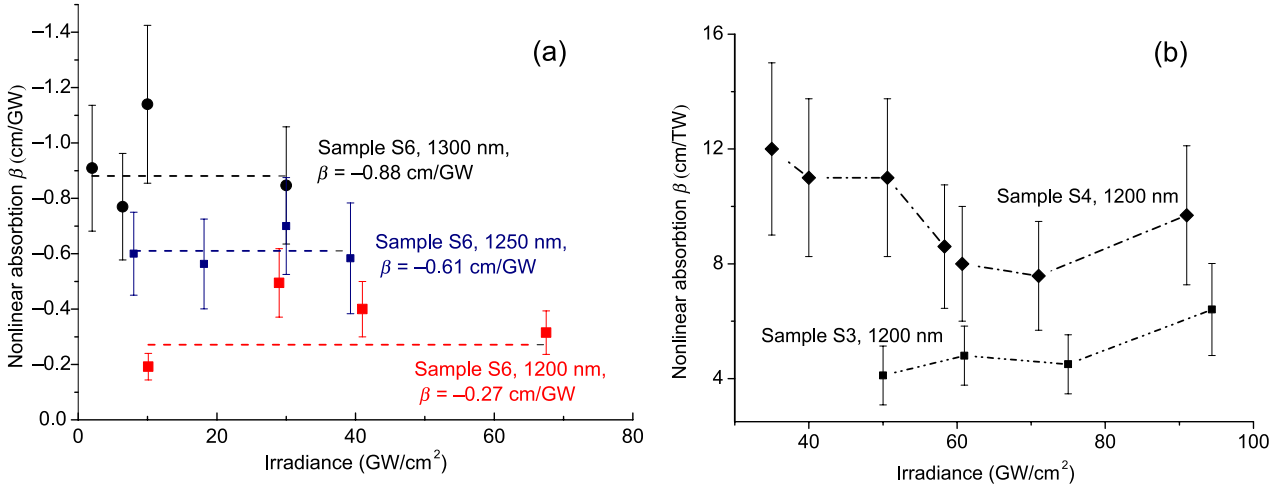

Fig. 4. Nonlinear absorption coefficient β associated with $\chi^{(3)}$ susceptibility Ag nanoprisms under different excitation regimes for sample S6 (a) and samples S3 and S4 (b). Error bar represents experimental uncertainty and lines are linear fits with a zero slope for (a) and serve as eye guidance for (b).

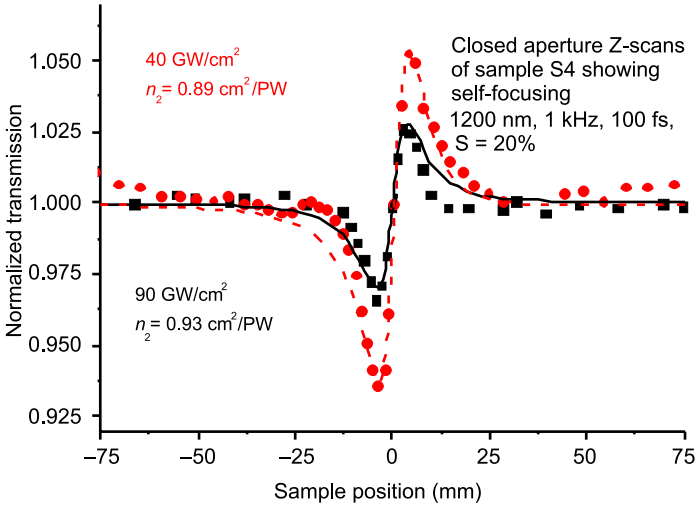

Fig. 5. Typical experimental close aperture transmission curves (dots) and theoretical fits (lines) of AgNP sample S4 at different beam intensities. The samples exibit positive nonlinear absorption (two-photon absorption) as well as positive nonlinear refraction (self-focusing). Beam characteristics: 100 fs, 1200 nm, 41 μm at 1/e^2.

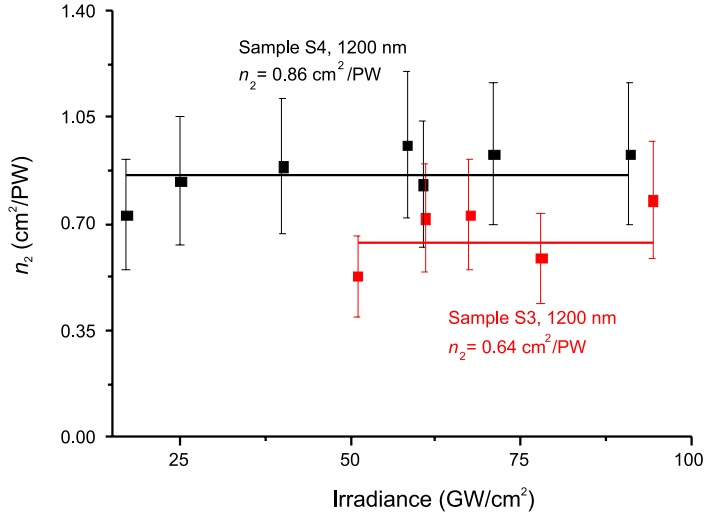

Fig. 6. $\chi^{(3)}$ associated nonlinear refraction n_2 coefficient in silver nanoprism samples S3 and S4 at the wavelength 1200 nm under different excitation regimes. Error bar represents experimental uncertainty mainly caused by beam intensity estimation. Lines are linear fits with a zero slope.

refraction. This type of refraction is also called self-focusing. The values of nonlinear index of refraction are positive and small (see Fig. 6), 0.64 cm^2/PW for sample S3 and 0.86 cm^2/PW for sample S4. Indexes do not show any variation when the irradiance is changed from 13 GW/cm^2 up to 80 GW/cm^2. These results accord with the results obtained in the report of Rativa et al. [36] as well as the model proposed by Hamanaka et al. [37]. According to their model, the nonlinear refraction arises from the creation of hot electrons and their intraband transitions and relaxation. When the exciting field wavelength is far from the main SPR of metal NPs, the nonlinear refractive index is small, and the refraction can be self-focusing.

Generally, the nonlinear refraction arises from the electronic effect or thermal mechanisms [25]. In the solution the thermal effect is a slow accumulative process which is associated with the non-radiative relaxation of the excitation energy gathered via linear or nonlinear absorption by the metal NPs. For the aqueous solution the buildup time of such thermal effect is about 30 ns [38], which is much longer than the duration of the laser pulse at 100 fs. In addition, the repetition rate of our laser and optical parametric amplifier tandem is 1 kHz, which is too low to accumulate heat. Therefore, the cause for the nonlinear refraction must be pure electronic effects.

Results also show that with increasing the silver nanoparticle size, the value of NLR coefficient n_2 associated with the third-order nonlinearity also increases. This fact could be explained considering the SPR absorption peak as the sample S4 absorption peak at 717 nm is nearer to the excitation wavelength compared to 636 nm for sample S3. Similar tendence was also obtained by Lama and co-workers for spherical shape silver nanoparticles, however, the sign of nonlinearity is doubtful, as the definition of the z axis in their calculation is not common [39].

It should be noted that nonlinear refraction for the samples with saturated absorption (S6 and S7) could not be properly determined by this method because of

Table 2. Comparison of our results on the nonlinear optical properties of nanoparticles with measurements of other groups.

Shape of Ag sample	Production method	Edge length (or other dimensions), nm	SPR peak wavelength (in plane dipole), nm	Measurement method and exciting laser field parameters	Nonlinear absorption coefficient, cm/GW	Nonlinear refraction coefficient, cm^2/GW	Source
Colloid of prisms in ethanol	Reduction of $AgNO_3$ by DMF in the presence of PVP [40]	67 × 35	496	Pump and probe, 100 fs, 400 nm as pump, WLC as probe, 0–15 GW/cm^2	0.06 at 540 nm –0.08 at 468 nm	–	[30]
Planar prism array	Nanosphere lithography	60 × 20	400	Degenerate Z-scan, 800 nm, 50 fs	Intensity dependent: 850 (at 55 GW/cm^2) –210 (at 280 GW/cm^2)	8.5 (at 55 GW/cm^2) –3.7 (at 280 GW/cm^2)	[41]
Prism suspension in water	Photo-induced method	Edge length: 40 to 80 Thickness: 8	740	Degenerate Z-scan, 735 nm, 2.5 ps, 76 MHz	from 0 to –3.2	from $0.6 \cdot 10^{-4}$ to $6.8 \cdot 10^{-4}$	[35]
Colloid of prisms in water	Two-step seed-mediated growth	52 × 5	717	Degenerate Z-scan, 100 fs, 1 kHz, 1200 nm, 0–100 GW/cm^2	0.01	$8.6 \cdot 10^{-7}$	this work
		45 × 4	636		0.005	$6.4 \cdot 10^{-7}$	
		39 × 4	570		0.001	–	
		190 × 10	1052		–0.27	–	

significant linear absorption, as well as increased data uncertainty caused by the division of CA over OA data.

The nonlinear refractions of Ag NPs have been reported by many researchers. Table 2 summarizes few numerous studies. These studies also contain different methods, however, most of them concentrate on the visible spectral region and generally cover regions near the SPR peak. To our knowledge, the results on nonlinearity of the silver nanoprism colloids in the near infrared spectral region have not yet been reported.

4. Conclusions

Using a two-step seed-mediated growth method we demonstrated that it is possible to synthesize different size and triangular shape silver nanoparticles, with their edge length ranging from 36 to 190 nm and with a thickness of several nanometres in an aqueous solution. Linear absorption spectra showed that the average silver nanoprism size and corresponding SPR peaks can be tuned in an exceptionally wide spectral range, however, distribution dispersion tends to increase with the chemical process time. Nanoprisms with dimensions of 52 × 5 nm are found to show positive nonlinear absorption, which was identified as two-photon absorption (0.01 cm/GW) and positive nonlinear refraction (self-focusing) of the order of 0.86 cm^2/PW in the NIR spectral region (1200 nm) under 30–100 GW/cm^2 femtosecond laser excitation. Nanoparticles with SPR peak nearer to the excitation wavelength (samples S5–S7) have negative nonlinear absorption and behave as saturable absorbers.

Acknowledgements

This study was partially funded by a student grant (DOK-13762) from the Research Council of Lithuania.

References

[1] R. Narayanan and M.A. El-Sayed, Catalysis with transition metal nanoparticles in colloidal solution: nanoparticle shape dependence and stability,

J. Phys. Chem. B **109**(26), 12663–12676 (2005), http://dx.doi.org/10.1021/jp051066p

[2] F. Hache, D. Ricard, and C. Flytzanis, Optical nonlinearities of small metal particles: surface-mediated resonance and quantum size effects, J. Opt. Soc. Am. B **3**(12), 1647–1655 (1986), http://dx.doi.org/10.1364/JOSAB.3.001647

[3] K.L. Kelly, C. Eduardo, Z. Lin Lin, E. Coronado, L.L. Zhao, and G.C. Schatz, The optical properties of metal nanoparticles: the influence of size, shape, and dielectric environment, J. Phys. Chem. B **107**, 668–677 (2003), http://dx.doi.org/10.1021/jp026731y

[4] R. Buividas, S. Rekštytė, M. Malinauskas, and S. Juodkazis, Nano-groove and 3D fabrication by controlled avalanche using femtosecond laser pulses, Opt. Mater. Express **3**(10), 1674–1686 (2013), http://dx.doi.org/10.1364/OME.3.001674

[5] M. Sheik-bahae, A.A. Said, and E.W. Van Stryland, High-sensitivity, single-beam n_2 measurements, Opt. Lett. **14**(17), 955–957 (1989).

[6] M. Chandra, S.S. Indi, and P.K. Das, Depolarized hyper-Rayleigh scattering from copper nanoparticles, J. Phys. Chem. C **111**(28), 10652–10656 (2007), http://dx.doi.org/10.1021/jp071847l

[7] S. Eustis and M.A. El-Sayed, Why gold nanoparticles are more precious than pretty gold: Noble metal surface plasmon resonance and its enhancement of the radiative and nonradiative properties of nanocrystals of different shapes, Chem. Soc. Rev. **35**(3), 209–217 (2005), http://dx.doi.org/10.1039/b514191e

[8] R.F. Haglund, R.H. Magruder, K. Becker, R.A. Zuhr, J.E. Wittig, and L. Yang, Picosecond nonlinear optical response of a Cu:silica nanocluster composite, Opt. Lett. **18**(5), 373–375 (1993), http://dx.doi.org/10.1364/OL.18.000373

[9] K. Uchida, S. Kaneko, S. Omi, C. Hata, H. Tanji, Y. Asahara, A.J. Ikushima, T. Tokizaki, and A. Nakamura, Optical nonlinearities of a high concentration of small metal particles dispersed in glass: copper and silver particles, J. Opt. Soc. Am. B **11**(7), 1236–1243 (1994), http://dx.doi.org/10.1364/JOSAB.11.001236

[10] T. Tokizaki, A. Nakamura, S. Kaneko, K. Uchida, S. Omi, H. Tanji, and Y. Asahara, Subpicosecond time response of third-order optical nonlinearity of small copper particles in glass, Appl. Phys. Lett. **65**(8), 941–943 (1994), http://dx.doi.org/10.1063/1.112155

[11] Y. Hong, Y.-M. Huh, S.S. Yoon, and J. Yang, Nanobiosensors based on localized surface plasmo+n resonance for biomarker detection, J. Nanomater. **2012** (2012), http://dx.doi.org/10.1155/2012/759830

[12] I.H. El-Sayed, X. Huang, and M.A. El-Sayed, Surface plasmon resonance scattering and absorption of anti-EGFR antibody conjugated gold nanoparticles in cancer diagnostics: applications in oral cancer, Nano Lett. **5**(5), 829–834 (2005), http://dx.doi.org/10.1021/nl050074e

[13] S. Eustis and M. El-Sayed, Aspect ratio dependence of the enhanced fluorescence intensity of gold nanorods: experimental and simulation study, J. Phys. Chem. B **109**(34), 16350–16356 (2005).

[14] T.K. Sau and C.J. Murphy, Room temperature, high-yield synthesis of multiple shapes of gold nanoparticles in aqueous solution, JACS **126**(28), 8648–8649 (2004), http://dx.doi.org/10.1021/ja047846d

[15] J.E. Millstone, S. Park, K.L. Shuford, L. Qin, G.C. Schatz, and C.A. Mirkin, Observation of a quadrupole plasmon mode for a colloidal solution of gold nanoprisms, JACS **127**(15), 5312–5313 (2005), http://dx.doi.org/10.1021/ja043245a

[16] B.D. Busbee, S.O. Obare, and C.J. Murphy, An improved synthesis of high-aspect-ratio gold nanorods, Adv. Mater. **15**(5), 414–416 (2003), http://dx.doi.org/10.1002/adma.200390095

[17] T.S. Ahmadi, Z.L. Wang, T.C. Green, A. Henglein, and M.A. El-Sayed, Shape-controlled synthesis of colloidal platinum nanoparticles, Science **272**(5270), 1924–1925 (1996).

[18] K.K. Caswell, C.M. Bender, and C.J. Murphy, Seedless, surfactantless wet chemical synthesis of silver nanowires, Nano Lett. **3**(5), 667–669 (2003), http://dx.doi.org/10.1021/nl0341178

[19] N.R. Jana, L. Gearheart, and C.J. Murphy, Wet chemical synthesis of silver nanorods and nanowires of controllable aspect ratio, Chem. Commun. **1**(7), 617–618 (2001), http://dx.doi.org/10.1039/B100521I

[20] Y. Sun, B. Mayers, and Y. Xia, Transformation of silver nanospheres into nanobelts and triangular nanoplates through a thermal process, Nano Lett. **3**(5), 675–679 (2003), http://dx.doi.org/10.1021/nl034140t

[21] S. Chen and D.L. Carroll, Synthesis and characterization of truncated triangular silver nanoplates, Nano Lett. **2**(9), 1003–1007 (2002), http://dx.doi.org/10.1021/nl025674h

[22] M.A. Correa-Duarte, J. Pérez-Juste, A. Sánchez-Iglesias, M. Giersig, and L.M. Liz-Marzán, Aligning Au nanorods by using carbon nanotubes as templates, Angew. Chem. Int. Ed. **44**(28), 4375–4378 (2005), http://dx.doi.org/10.1002/anie.200500581

[23] R. Jin, Y. Cao, C.A. Mirkin, K.L. Kelly, G.C. Schatz, and J.G. Zheng, Photoinduced conversion of silver nanospheres to nanoprisms, Science **294**(5548), 1901–1903 (2001), http://dx.doi.org/10.1126/science.1066541

[24] J.E. Millstone, G.S. Métraux, and C.A. Mirkin, Controlling the edge length of gold nanoprisms via a seed-mediated approach, Adv. Funct. Mater. **16**(9), 1209–1214 (2006), http://dx.doi.org/10.1002/adfm.200600066

[25] M. Sheik-Bahae, A.A. Said, T.-H. Wei, D.J. Hagan, and E.W.V. Stryland, Sensitive measurement of optical nonlinearities using a single beam, IEEE J. Quantum Electron. **26**(4), 760–769 (1990).

[26] P.B. Chapple, J. Staromlynska, J.A. Hermann, and T.J. Mckay, Single-beam Z-scan: measurement techniques and analysis, J. Nonlinear Opt. Phys. Mater. **6**(3), 251–293 (1997).

[27] T. Xia, D.J. Hagan, M. Sheik-Bahae, and E.W. Van Stryland, Eclipsing Z-scan measurement of $\lambda/10^4$ wave-front distortion, Opt. Lett. **19**(5), 317–319 (1994).

[28] E.W. Van Stryland and M. Sheik-Bahae, in: *Characterization Techniques and Tabulations for Organic Nonlinear Materials*, eds. M.G. Kuzyk and C.W. Dirk (Marcel Dekker, 1998) pp. 655–692.

[29] M. Sheik-Bahae and M.P. Hasselbeck, in: *OSA Handbook of Optics*, Vol. 4 (McGraw-Hill, 2001) pp. 17.13–17.38.

[30] N. Okada, Y. Hamanaka, A. Nakamura, I. Pastoriza-Santos, and L.M. Liz-Marzán, Linear and nonlinear optical response of silver nanoprisms: local electric fields of dipole and quadrupole plasmon resonances, J. Phys. Chem. B **108**(26), 8751–8755 (2004), http://dx.doi.org/10.1021/jp048193q

[31] L.J. Sherry, R. Jin, C.A. Mirkin, G.C. Schatz, and R.P. Van Duyne, Localized surface plasmon resonance spectroscopy of single silver triangular nanoprisms, Nano Lett. **6**(9), 2060–2065 (2006), http://dx.doi.org/10.1021/nl061286u

[32] U. Gurudas, E. Brooks, D.M. Bubb, S. Heiroth, T. Lippert, and A. Wokaun, Saturable and reverse saturable absorption in silver nanodots at 532 nm using picosecond laser pulses, J. Appl. Phys. **104**(7), 073107–073108 (2008).

[33] F. Guang-Hua, Q. Shi-Liang, G. Zhong-Yi, W. Qiang, and L. Zhong-Guo, Size-dependent nonlinear absorption and refraction of Ag nanoparticles excited by femtosecond lasers, Chin. Phys. B **21**(4), 047804 (2012).

[34] T. Cesca, P. Calvelli, G. Battaglin, P. Mazzoldi, and G. Mattei, Nonlinear optical response of gold–silver nanoplanets, Radiat. Eff. Defect. Solids **167**(7), 520–526 (2012), http://dx.doi.org/10.1080/10420150.2012.680458

[35] X. Wang, F. Nan, S. Liang, L. Zhou, and Q. Wang, Optical properties of silver nanoplates synthesized by photoinduced method, Wuhan Univ. J. Nat. Sci. **18**(3), 201–206 (2013), http://dx.doi.org/10.1007/s11859-013-0915-y

[36] D. Rativa, R.E. de Araujo, and A.S. Gomes, One photon nonresonant high-order nonlinear optical properties of silver nanoparticles in aqueous solution, Opt. Express **16**(23), 19244–19252 (2008), http://dx.doi.org/10.1364/OE.16.019244

[37] Y. Hamanaka, A. Nakamura, N. Hayashi, and S. Omi, Dispersion curves of complex third-order optical susceptibilities around the surface plasmon resonance in Ag nanocrystal–glass composites, J. Opt. Soc. Am. B **20**(6), 1227–1232 (2003), http://dx.doi.org/10.1364/JOSAB.20.001227

[38] G. Fan, S. Qu, Q. Wang, C. Zhao, L. Zhang, and Z. Li, Pd nanoparticles formation by femtosecond laser irradiation and the nonlinear optical properties at 532 nm using nanosecond laser pulses, J. Appl. Phys. **109**(2), 023102 (2011), http://dx.doi.org/10.1063/1.3533738

[39] P. Lama, A. Suslov, A.D. Walser, and R. Dorsinville, Plasmon assisted enhanced nonlinear refraction of monodispersed silver nanoparticles and their tunability, Opt. Express **22**(11), 14014–14021 (2014), http://dx.doi.org/10.1364/OE.22.014014

[40] I. Pastoriza-Santos and L.M. Liz-Marzán, Synthesis of silver nanoprisms in DMF, Nano Lett. **2**(8), 903–905 (2002), http://dx.doi.org/10.1021/nl025638i

[41] B.-H. Yu, D.-L. Zhang, Y.-B. Li, and Q.-B. Tang, Nonlinear optical behaviors in a silver nanoparticle array at different wavelengths, Chin. Phys. B **22**(1), 014212 (2013), http://dx.doi.org/10.1088/1674-1056/22/1/014212

SIDABRO NANODALELIŲ OPTINIAI NETIESIŠKUMAI, IŠTIRTI NAUDOJANT Z SKENAVIMO METODIKĄ SU FEMTOSEKUNDINIAIS LAZERINIAIS IMPULSAIS

A. Alesenkov [a], J. Pilipavičius [b], A. Beganskienė [b], R. Sirutkaitis [c], V. Sirutkaitis [a]

[a] *Vilniaus universiteto Lazerinių tyrimų centras, Vilnius, Lietuva*

[b] *Vilniaus universiteto Neorganinės chemijos katedra, Vilnius, Lietuva*

[c] *Vilniaus universiteto Biochemijos institutas, Vilnius, Lietuva*

Santrauka

Straipsnyje pristatomos nanokompozitinės medžiagos, susidedančios iš sidabro nanoprizmių, disperguotų distiliuotame vandenyje, tyrimų rezultatai. Suspensija buvo pagaminta dviejų žingsnių cheminiu procesu naudojant užkratą. Nanodalelių sugerties spektras parodė išreikštas plazmonines dalelių savybes. Didėjant prizmių kraštinei nuo 20 iki 150 nm, sugerties smailė slinko link ilgesnių bangos ilgių spektriniame diapazone tarp 400 ir 1100 nm. Žadinant nanodaleles didelio intensyvumo femtosekundiniais lazeriniais impulsais infraraudonojoje spektro dalyje (1200–1400 nm), medžiagoje buvo stebėti netiesiniai optiniai reiškiniai, pavyzdžiui, praskaidrėjimas, dvifotonė sugertis ir fokusavimas.